11th World Congress on Computational Mechanics (WCCM XI)
5th European Conference on Computational Mechanics (ECCM V)
6th European Conference on Computational Fluid Dynamics (ECFD VI)
E. Oñate, J. Oliver and A. Huerta (Eds)

MULTISCALE MODELING OF PROGRESSIVE DAMAGE IN ELASTO-PLASTIC COMPOSITE MATERIALS

JOHANNES SPAHN[*,†], HEIKO ANDRAE[*], MATTHIAS KABEL[*], RALF MUELLER[†] AND CHRISTIAN LINDER[#]

[*] Fraunhofer Institute for Industrial Mathematics (ITWM)
Department Flow and Material Simulation
Fraunhofer-Platz 1, 67663 Kaiserslautern, Germany
e-mail: spahn@itwm.fraunhofer.de, web page: http://www.itwm.fraunhofer.de

[†]Institute of Applied Mechanics
Technische Universität Kaiserslautern
Gottlieb-Daimler-Straße, 67653 Kaiserslautern, Germany

[#]Department of Civil and Environmental Engineering
Stanford University, 473 Via Ortega, Stanford, CA 94305, USA

Key words: Multiscale Analysis, Computational Homogenization, Continuum Damage Mechanics, Fast Fourier Transforms, Composite Materials

Abstract. Conventional macro mechanical models and closed form estimates are in many cases not sufficient to appropriately predict the mechanical material response of composite materials. Composite failure occurs as a result of complex microstructural damage mechanisms. In this contribution we propose an alternative approach, non-linear material effects caused by progressive damage behavior are captured directly on a finer scale and the microstructural constituents are modeled explicitly. In contrast to conventional methods, which resort to the Finite Element Method (FEM), the boundary value problem is reformulated into an integral equation of Lippmann-Schwinger type and solved more efficiently using Fast Fourier Transforms (FFT). In the work at hand, a ductile damage model and an equivalent microscopic boundary value problem are described. The numerical method is validated with experimental data for a thermoplastic composite material.

1 INTRODUCTION

In many practicable applications phenomenological macroscale models are used for the investigation of failure. In order to avoid the extensive identification of material parameters in dependence of the material structure and the loading conditions the non-linear material effects can be captured directly on a finer scale. Analytical methods

based on closed form estimates consider the micromechanical structure of the material by means of analytical approximations. These methods are usually restricted to certain inclusion shapes [1] and the interactions between inclusions are only captured to a certain degree. Frequently, the occurrence of micro cracks is ignored. Progressive damage is usually modeled by empirical failure criteria. To overcome these shortcomings one has to perform direct or full-field simulations. The microstructural constituents are modeled explicitly on the interesting scale instead of forming effective constitutive equations. The resulting material response is based on genuine physical effects, and consequently arbitrary complex non-proportional, multiaxial loading conditions can be captured. Due to the increased computational costs coming along with the fine discretization of the microstructure an effective solution of the micro boundary value problem (μBVP) is necessary. In this work, we use Fast Fourier Transforms (FFT) to solve an equivalent elastic μBVP formulation, the so called Lippmann-Schwinger equation. Advantages of this method proposed by [2] are its efficiency in terms of memory consumption and computational time. The calculation is carried out on a regular voxel grid which can be obtained from 3D images like tomographies without using any complicated mesh generation. The behavior of the constituents is isotropic and the required material parameters are obtained from a standard cyclic tensile test. In Section 2 the elasto-plastic damage law is introduced and the equivalent boundary value problem is formulated in Section 3. In Section 4 the simulated results are validated with experimental data for a short fiber reinforced thermoplastic material.

2 ELASTOPLASTICITY COUPLED WITH DAMAGE

Ductile materials, like e.g. thermoplastic polymers, show damage and plasticity at the same time. Thus, a coupled constitutive law describing the interaction between the processes is necessary. In this work, a modified model of Ju [3] is used to define the ductile material degradation. The damage variable d is defined by the relation of the damaged area A_d to the initial area A_0 in a cross section of the material

$$d = \frac{A_d}{A_0} \, . \tag{1}$$

Further, the concept of effective stress is introduced, which sets the nominal stress $\boldsymbol{\sigma}$ in relation with the (higher) effective stress

$$\bar{\boldsymbol{\sigma}} = \boldsymbol{\sigma}/(1-d) \, , \tag{2}$$

which would act in an undamaged material cross section. Models using this concept are mainly based on the principle of strain equivalence which states that the effective strain $\bar{\boldsymbol{\varepsilon}}$ equals the real strain $\boldsymbol{\varepsilon}$. For details on damage mechanics also see [4]. The state laws are derived from an energy potential, the Helmholtz free energy ψ.

The free energy is decomposed into an elastic and into a plastic part, i.e.

$$\psi(\boldsymbol{\varepsilon}_e, d, r) \;=\; \psi_e(\boldsymbol{\varepsilon}_e, d) + \psi_p(d, r) = \frac{1}{2}(1-d)\;\left(\boldsymbol{\varepsilon}_e : \mathbb{C}_\mathrm{e} : \boldsymbol{\varepsilon}_e + \psi_p(r)\right)\;, \tag{3}$$

and thus, the state laws are obtained in the following form:

$$\begin{aligned} \boldsymbol{\sigma} &= \frac{\partial \psi}{\partial \boldsymbol{\varepsilon}_e} = (1-d)\;\mathbb{C}_\mathrm{e} : \boldsymbol{\varepsilon}_e\;, \\ Y = -\frac{\partial \psi}{\partial d} &= \frac{1}{2}\;\boldsymbol{\varepsilon}_e : \mathbb{C}_\mathrm{e} : \boldsymbol{\varepsilon}_e + \psi_p(r)\;, \quad R = -\frac{\partial \psi}{\partial r}\;. \end{aligned} \tag{4}$$

In the definitions above, Y is the strain energy of the undamaged material as the work conjugated force to d, the driving force R is conjugate to the isotropic hardening variable r. The evolution laws of the internal variables are derived from two independent dissipation potentials F_p and F_d and two independent multipliers $\dot{\lambda}_p$ and $\dot{\lambda}_d$. Furthermore, both mechanisms are controlled by two independent criteria f_p and f_d

$$f_p(\boldsymbol{\sigma}, R, d) \leq 0\;, \quad F_p = f_p(\boldsymbol{\sigma}, R, d) \qquad\qquad f_d(Y, d) \leq 0\;, \quad F_d(Y, d)\;, \tag{5}$$

$$\dot{\boldsymbol{\varepsilon}}_p = \dot{\lambda}_p\;\frac{\partial f_p}{\partial \boldsymbol{\sigma}}\;, \quad \dot{r} = -\dot{\lambda}_p\;\frac{\partial f_p}{\partial R} \qquad\qquad \dot{d} = \dot{\lambda}_d\;\frac{\partial F_d}{\partial Y}\;, \tag{6}$$

where the potential F_d is replaced by a set of piecewise linear functions for interpolating between discrete measured points, see Section 4. The plastic flow is determined by a von Mises type yield function which is evaluated in the effective stress space

$$f_p(\boldsymbol{\sigma}, R; d) = f_p(\bar{\boldsymbol{\sigma}}, R) = \frac{\sigma_{eq}}{1-d} - \sigma_Y - R \leq 0\;, \tag{7}$$

where σ_{eq} is the equivalent von Mises stress. The damage criterion is characterized by a damage threshold in terms of a current energy barrier that limits the elastic domain

$$f_d(Y; d) = Y(t) - \max_{-\infty<\tau<t}\{Y\}\;. \tag{8}$$

The computational algorithm for the integration of the elasto-plastic damage evolution is straightforward and efficient. It consists of three independent steps:

1. Elastic predictor
2. Plastic corrector
3. Damage corrector

This approach allows to establish independent relations for plasticity and damage. Both mechanisms are coupled only by the effective stress concept in the plastic yield criterion.

3 Equivalent BVP and FFT-based Numerical Solution

In this work, an equivalent formulation of the homogenization problem is used to obtain effective material quantities of a unit cell problem. The governing differential equation that describes the elastic boundary value problem is reformulated into an integral equation of Lippmann-Schwinger type [5] and solved in the Fourier space. In general, the following constitutive equation defines the non-linear stress-strain relation:

$$\boldsymbol{\sigma}(\boldsymbol{x}) = \mathcal{F}\left(\boldsymbol{\varepsilon}(\boldsymbol{x}), \boldsymbol{\varepsilon}_p(\boldsymbol{x}), r(\boldsymbol{x}), d(\boldsymbol{x})\right) \ , \tag{9}$$

where the dependence of the constitutive equation $\mathcal{F}$ on the internal history variables is indicated by $(\boldsymbol{\varepsilon}_p(\boldsymbol{x}), r(\boldsymbol{x}), d(\boldsymbol{x}))$. For computing the effective quantities of a periodic medium with local stiffness $\mathbb{C}(\boldsymbol{x})$ a cubic RVE $\omega \,\text{in}\, \mathbb{R}^3$ with periodic boundary conditions on $\partial\omega$ is considered. The local strain field is decomposed into a prescribed constant macroscopic strain $\boldsymbol{E}$ and a fluctuation term $\boldsymbol{\varepsilon}(\boldsymbol{u}^*(\boldsymbol{x}))$.

$$\begin{aligned}
\operatorname{div} \boldsymbol{\sigma}(\boldsymbol{x}) &= \boldsymbol{0} && \forall\, \boldsymbol{x} \,\text{in}\, \omega \ , && \text{(10a)}\\
\boldsymbol{\sigma}(\boldsymbol{x}) &= \mathcal{F}\left(\boldsymbol{\varepsilon}(\boldsymbol{x}), \boldsymbol{\varepsilon}_p(\boldsymbol{x}), r(\boldsymbol{x}), d(\boldsymbol{x})\right) && \forall\, \boldsymbol{x} \,\text{in}\, \omega \ , && \text{(10b)}\\
\boldsymbol{\varepsilon}(\boldsymbol{x}) &= \boldsymbol{E} + \tfrac{1}{2}\left(\bigtriangledown \boldsymbol{u}^*(\boldsymbol{x}) + (\bigtriangledown \boldsymbol{u}^*(\boldsymbol{x}))^T\right) && \forall\, \boldsymbol{x} \,\text{in}\, \omega \ , && \text{(10c)}\\
\boldsymbol{u}^*(\boldsymbol{x}) &\quad \text{periodic} && \forall\, \boldsymbol{x} \,\text{on}\, \partial\omega \ , && \text{(10d)}\\
\boldsymbol{\sigma}(\boldsymbol{x}) \cdot \boldsymbol{n}(\boldsymbol{x}) &\quad \text{anti-periodic} && \forall\, \boldsymbol{x} \,\text{on}\, \partial\omega \ . && \text{(10e)}
\end{aligned}$$

According to Zeller and Dederichs [6] the differential equation (10a) can be reformulated in an integral equation, the so called Lippmann-Schwinger equation. By introducing a homogeneous reference material with the stiffness $\mathbb{C}^0$, the polarization stress $\boldsymbol{\tau}$ with respect to this reference material reads as follows:

$$\boldsymbol{\tau}(\boldsymbol{x}) = \boldsymbol{\sigma}(\boldsymbol{x}) - \mathbb{C}^0 : \boldsymbol{\varepsilon}(\boldsymbol{x}) \ . \tag{11}$$

The solution of the local problem in equation (10) can now be obtained using a nonlocal Green operator $\boldsymbol{\Gamma}^0$ which is applied on the stress polarization $\boldsymbol{\tau}$

$$\boldsymbol{\varepsilon}(\boldsymbol{x}) = \boldsymbol{E} - \int_\omega \boldsymbol{\Gamma}^0(\boldsymbol{x}, \boldsymbol{y}) : \boldsymbol{\tau}(\boldsymbol{x}) \, \mathrm{d}\boldsymbol{y} \ . \tag{12}$$

The convolution integral in equation (12) transforms in the Fourier space into a multiplication and the corresponding relation reads:

$$\hat{\boldsymbol{\varepsilon}}(\boldsymbol{\xi}) = -\hat{\boldsymbol{\Gamma}}^0(\boldsymbol{\xi}) : \hat{\boldsymbol{\tau}}(\boldsymbol{\xi}), \quad \forall \boldsymbol{\xi} \neq \boldsymbol{0},\ \hat{\boldsymbol{\varepsilon}}(\boldsymbol{0}) = \boldsymbol{E} \ , \tag{13}$$

where $\hat{f}(\cdot)$ denotes a function in the Fourier space and $\boldsymbol{\xi}$ is the Fourier space variable corresponding to the coordinates $\boldsymbol{x}$.
The Green operator $\boldsymbol{\Gamma}^0$ is only associated with the stiffness of the homogenous linear

elastic reference material $\mathbb{C}^0$ and the given boundary conditions, but does not depend on the fluctuating quantities [7]. For an isotropic reference material the Fourier transform of the Green operator $\hat{\mathbf{\Gamma}}^0$ is explicitly known [2].
In this work, the so called basic scheme is used to solve the Lippmann-Schwinger integral equation iteratively, which was introduced by Moulinec and Suquet [2]. The transformation of the calculated fields is performed by the (discrete) Fast Fourier Transformation (FFT). The problem is solved by a fixed-point iteration and in each iteration the following four steps of the basic scheme are executed:

1. Solve the constitutive equation in the real space
   $\boldsymbol{\tau}^i = \boldsymbol{\sigma}\left(\boldsymbol{\varepsilon}^i, ...\right) - \mathbb{C}^0 : \boldsymbol{\varepsilon}^i$
2. Fourier transformation of the stress polarization field
   $\hat{\boldsymbol{\tau}}^i = \mathrm{FFT}(\boldsymbol{\tau}^i)$
3. Convolution with the Green operator in the Fourier space
   $\hat{\boldsymbol{\varepsilon}}^{i+1} = -\hat{\mathbf{\Gamma}}^0 : \hat{\boldsymbol{\tau}}^i, \quad \hat{\boldsymbol{\varepsilon}}^{i+1}(0) = \boldsymbol{E}$
4. Inverse Fourier transformation of the updated strain field
   $\boldsymbol{\varepsilon}^{i+1} = \mathrm{FFT}^{-1}(\hat{\boldsymbol{\varepsilon}}^{i+1})$

According to [2] convergence is reached when the global stress field is in equilibrium:

$$\frac{\|\mathrm{div}\ \boldsymbol{\sigma}^{i+1}\|^2}{\|\boldsymbol{\sigma}^{i+1}\|^2} \leq \ \mathrm{tol}\,, \tag{14}$$

which can easily be computed in the Fourier space:

$$\frac{\left\|\boldsymbol{\xi} \cdot \hat{\boldsymbol{\sigma}}^{i+1}(\boldsymbol{\xi})\right\|^2}{\left\|\hat{\boldsymbol{\sigma}}^{i+1}(\mathbf{0})\right\|^2} \leq \mathrm{tol}\,. \tag{15}$$

Thereby $\hat{\boldsymbol{\sigma}}(\mathbf{0})$ equals the average or macroscopic stress and $\|\cdot\|^2$ denotes the L^2 norm of the appropriate field variable. A typical value for the convergence tolerance is $\mathrm{tol} = 10^{-5}$.

In the last decade certain numerical schemes were developed to improve the convergence behavior of the FFT method for materials with high stiffness contrasts or non-linear behavior. A review of different schemes and an analysis of the convergence behavior for the computation of precise bounds of effective properties in comparison with analytical estimates can be found in [8]. As far as no convergence problems occurred, the basic scheme is used to compute the examples in this work. The coupled elasto-plastic damage model described in Section 2 is implemented in the framework of a three dimensional FFT-based elasticity solver.

4 VALIDATION WITH EXPERIMENTAL TENSILE TESTS

Within this example a modified form of the elasto-plastic damage model of Ju [3] introduced in Section 2 is used to simulate the mechanical behavior of a short fiber reinforced injection-molded composite material. The experimental data were taken from Hoffmann [9] and were kindly provided by the Robert Bosch GmbH in digital form. The material under consideration is polybutylene terephthalate (PBT) and E-glass fibers of 30 % mass fraction. The Young's modulus of the fibers is $E = 72$ GPa and the value for the polymer matrix material is $E = 2.5$ GPa.

4.1 Parameter Identification of the Elasto-Plastic Matrix Material

The non-linear parameters of the matrix material model are obtained by a uniaxial cyclic tensile test. The yield stress σ_Y, the irreversible plastic strain ε_p as the residual

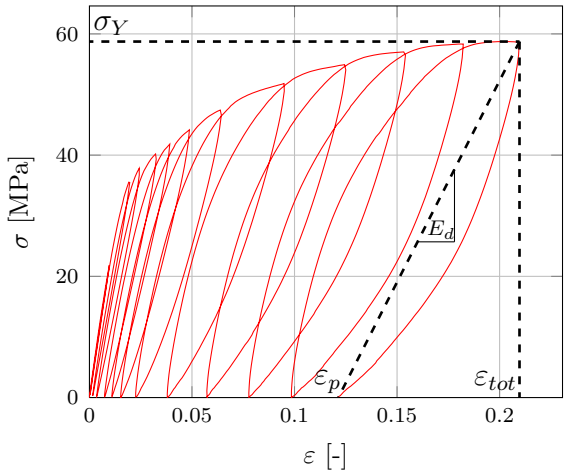

Figure 1: Material parameter identification with the experimental cyclic stress-strain response of the thermoplastic matrix material.

cycle	σ_Y [MPa]	$\varepsilon_p[-]$	$d[-]$	$\varepsilon_{tot}[-]$
1	44.64	0.0065	0.322	0.0328
2	51.36	0.0218	0.519	0.0645
3	56.34	0.0391	0.599	0.0953
4	58.78	0.0562	0.659	0.1252
5	60.38	0.0779	0.683	0.1542
6	61.88	0.1001	0.699	0.1823
7	62.68	0.1224	0.713	0.2097

Table 1: Identified material parameters of the thermoplastic matrix material for the elasto-plastic damage model.

strain at zero stress and the damage variable d are obtained for each load cycle from the stress-strain diagram shown in Figure 1. The degradation of the elastic modulus E_d, which is obtained in the unloading regime, gives the damage variable d within the following expression:

$$d = 1 - \frac{E_d}{E_0} \qquad E_d = \frac{\sigma_Y}{\varepsilon_{tot} - \varepsilon_p} = \frac{\sigma_Y}{\varepsilon_e} \,, \tag{16}$$

where ε_{tot} and ε_e are the total and the reversible elastic strain, respectively. The measured parameters are listed in Table 1 for seven load cycles.

4.2 Validation of the Matrix Material

The elasto-plastic material behavior introduced in Section 2 is implemented in a 3D FFT-based solver. Using linear interpolation of the measured tabular values listed in Table 1 to define the material behavior proved to be the most simple and accurate way to reproduce the experimental results. The cyclic tensile test is carried out at a single voxel structure. The resulting stress-strain curve is depicted in Figure 2. The non-linear

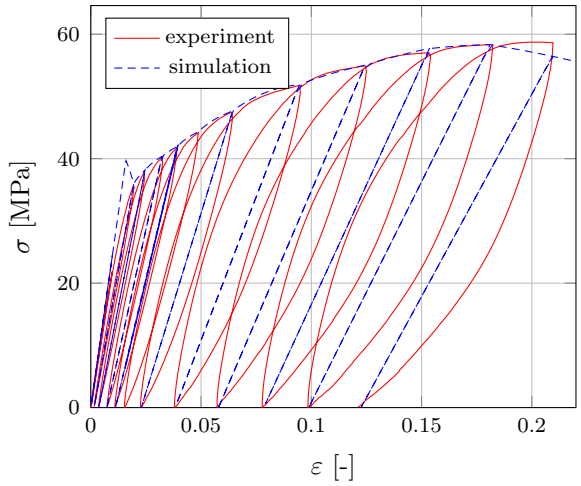

Figure 2: Experimental and simulated cyclic stress-strain response of the matrix material.

stress-strain behavior, the residual plastic strain as well as the degraded Young's modulus are well predicted by the computational model. Due to the fact that kinematic hardening is neglected in the plastic material law, the hysteresis loops of the experimental curves are not captured.

4.3 RVE Generation of the Composite Material

For the simulation of the composite material behavior, representative unit cells were created. Length, diameter and volume fraction of the fibers are chosen according to measured data. The RVEs are decomposed in three thickness layers with different fiber orientations. A realization of the RVE is illustrated in Figure 5. In the following tensile tests are shown in variation of the loading direction $\boldsymbol{n} = (\cos\varphi, \sin\varphi, 0)$, namely in $\varphi = 0°$, $45°$ and $90°$ with respect to the main fiber orientation.

4.4 Elastic Properties of the Composite Material

In the first validation step the elastic properties of the RVE are tested by defining linear elastic material parameters for fiber and matrix material. The elastic stiffness tensor is obtained during a numerical homogenization process, by applying six mechanical load cases (see [10, 11] for more details). Hence, the directional dependent Young's

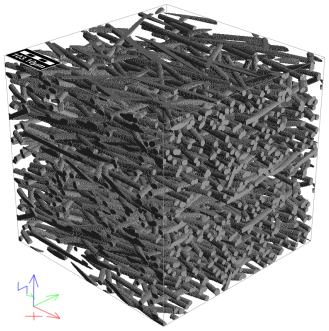

Figure 3: RVE structural setting with three fiber orientation layers over the thickness.

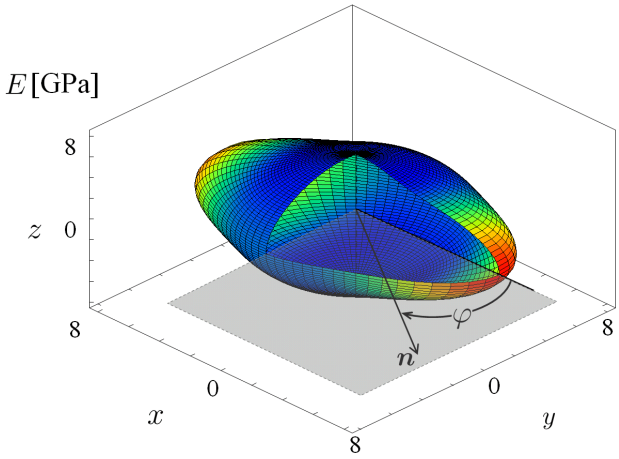

Figure 4: Graphical representation of the directional dependent Young's modulus $E(\boldsymbol{n})$.

modulus $E(\boldsymbol{n})$ can be represented as a function of the loading direction $\boldsymbol{n}$, see Figure 6. Simulated and measured values of the Young's modulus for different directions in the xy-plane are depicted in Figures 7 and 8. Simulated and experimental values show very

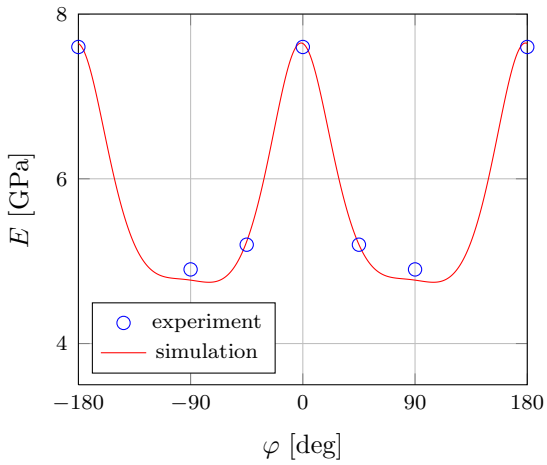

Figure 5: Experimental and simulated Young's modulus over loading angle φ in the xy-plane..

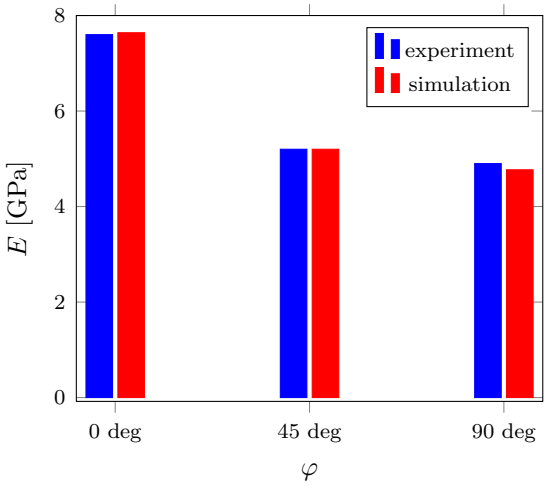

Figure 6: Experimental and simulated Young's modulus for different loading angles φ in the xy-plane.

good agreement, which indicates that the anisotropy of the elastic constants are captured very accurately by the microstructural setting.

4.5 Monotonic Non-linear Properties of the Composite Material

In the following, monotonic tensile tests for the different loading directions are compared to experimental results. While the non-linear material behavior of the thermoplastic

matrix material is modeled with the elasto-plastic material model, the fibers are assumed to behave linearly elastic. Experimental and simulated results for each direction are illustrated in Figure 9. The simulated stress-strain curves agree well with the measured

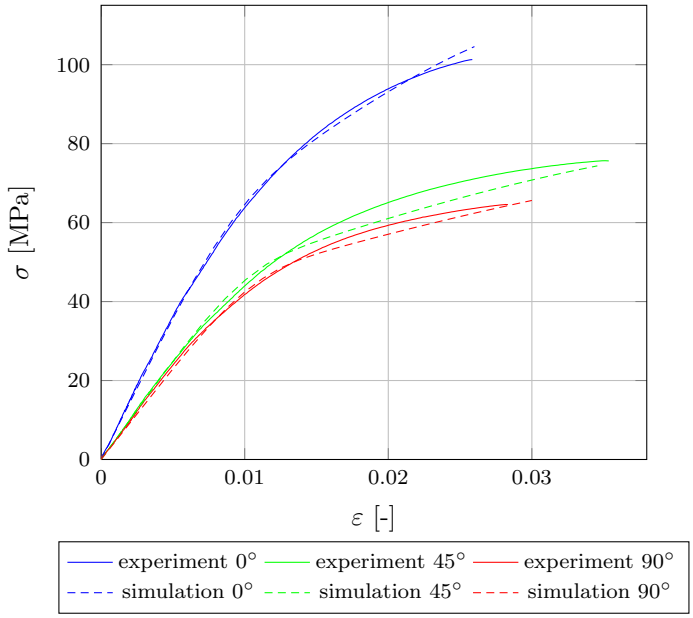

Figure 7: Experimental and simulated stress-strain curves for different loading angles φ.

ones. The linear elastic behavior and the transition to a non-linear stress-strain regime are captured nearly perfectly. Fiber breakage is not taken into account and hence, the slope of the curve for the 0° simulation is too high at the very end. In Figures 10 and 11 the distribution of the damage variable and plastic strain are shown for the different loading directions.

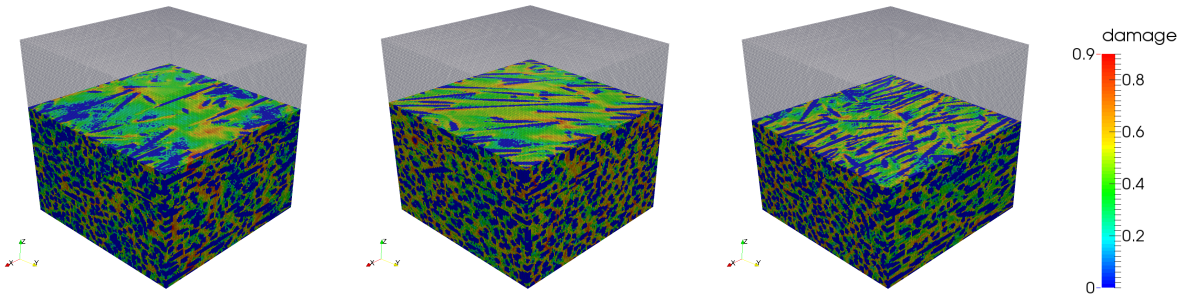

Figure 8: Damage fields after monotonic loading for the 0°(left), 45°(middle) and 90°(right) direction.

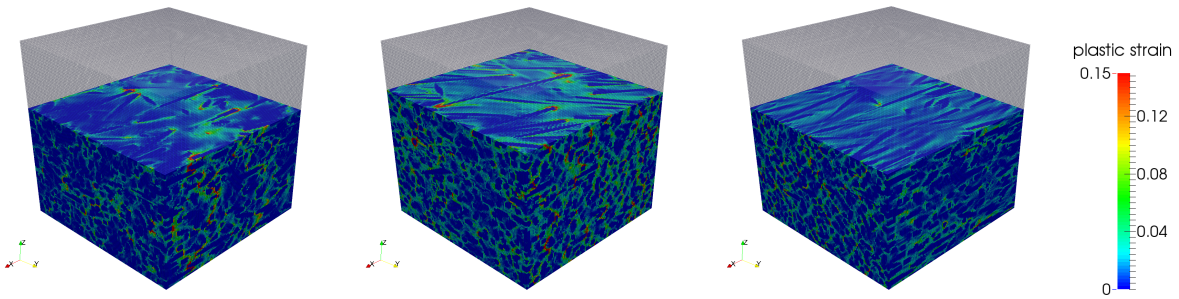

Figure 9: Distribution of the equivalent plastic strain after monotonic loading for the 0°(left), 45°(middle) and 90°(right) direction.

4.6 Cyclic Non-linear Properties of the Composite Material

In cyclic tensile tests the loading/unloading behavior of the composite material is simulated in the three different directions. The resulting stress-strain curves are displayed in Figure 12. The simulated curves show a very good agreement with the experimental data. Residual strain and the degraded stiffness are captured very well, especially for the 0° and 45° samples. The enveloping stress-strain curves, particularly the ones of the 0° and 90° samples, present a very similar behavior as the experimental results. Due to the negligence of fiber breakage, the model behavior is always approximated too stiff in the regime of pronounced strains near fracture.

5 CONCLUSIONS

In this contribution the prediction of non-linear composite properties is shown based on a microstructural model. The geometrical setting is obtained from micrograph analysis. Using material parameters for the matrix material obtained from a standard cyclic tensile test, the matrix material behavior can be reproduced easily. Besides the elastic parameters for the glass fibers no further material parameters have been defined. The effective response of the composite follows directly from the material laws of the constituents, and the geometry of the microstructural model. With this effective numerical homogenization approach even unloading tests are reproduced correctly in different loading directions. Reproducing these results would be hardly possible with analytical or semi-analytical homogenization approaches; especially when non-proportional load paths are taken into consideration. This contribution is restricted to the effective micromechanical behavior, but the micromechanical method can easily be coupled with a macroscopic problem. In [10] a FE^2-like approach is shown which considers by means of a fully coupled micro-macro simulation process different length scales of the material structure. Modeling solids at failure on multiple scales by the strong discontinuity approach [12] was proposed in [13].

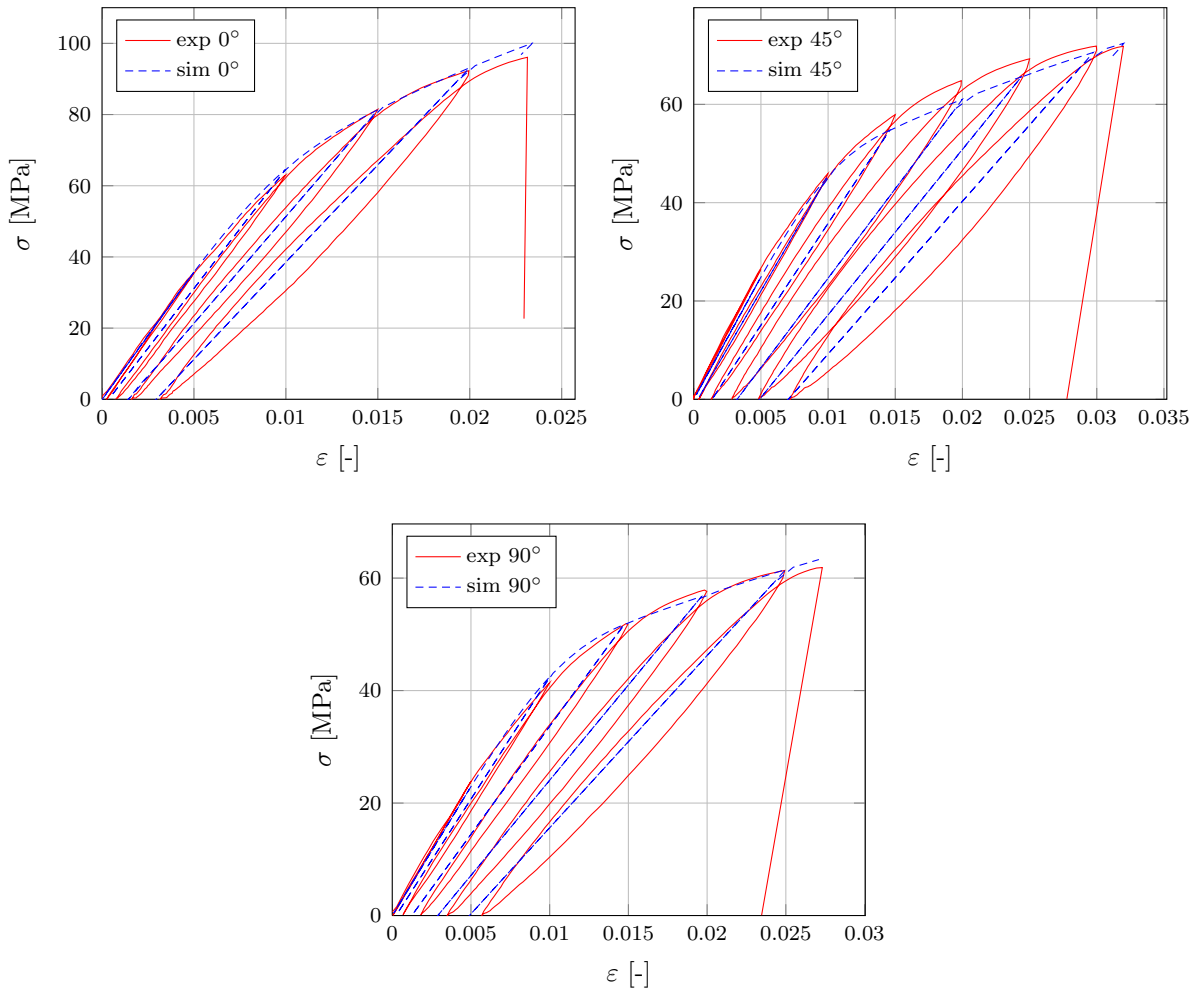

Figure 10: Experimental and simulated cyclic stress-strain curves in different loading directions.

REFERENCES

[1] B Klusemann, HJ Böhm, and B Svendsen. Homogenization methods for multi-phase elastic composites with non-elliptical reinforcements: Comparisons and benchmarks. *European Journal of Mechanics-A/Solids*, 34:21–37, 2012.

[2] H Moulinec and P Suquet. A numerical method for computing the overall response of nonlinear composites with complex microstructure. *Computer Methods in Applied Mechanics and Engineering*, 157(1):69–94, 1998.

[3] JW Ju. On energy-based coupled elastoplastic damage theories: constitutive modeling and computational aspects. *International Journal of Solids and Structures*, 25(7):803–833, 1989.

[4] L Kachanov. *Introduction to continuum damage mechanics*, volume 10. Springer, 1986.

[5] BA Lippmann and J Schwinger. Variational principles for scattering processes. I. *Physical Review*, 79(3):469–480, 1950.

[6] R Zeller and PH Dederichs. Elastic constants of polycrystals. *Physica status solidi (b)*, 55(2):831–842, 1973.

[7] E Kröner. Bounds for effective elastic moduli of disordered materials. *Journal of the Mechanics and Physics of Solids*, 25(2):137–155, 1977.

[8] M Kabel and H Andrä. Numerical bounds of effective elastic moduli. *Berichte des Fraunhofer ITWM*, 224(1):1–13, 2012.

[9] S Hoffmann. *Computational Homogenization of Short Fiber Reinforced Thermoplastic Materials*. University Kaiserslautern, LTM, 2012.

[10] J Spahn, H Andrä, M Kabel, and R Müller. A multiscale approach for modeling progressive damage of composite materials using fast Fourier transforms. *Computer Methods in Applied Mechanics and Engineering*, 268:871–883, 2014.

[11] J Spahn. *An efficient multiscale method for modeling progressive damage in composite materials*. PhD thesis, University Kaiserslautern, LTM, submitted.

[12] C Linder and F Armero. Finite elements with embedded strong discontinuities for the modeling of failure in solids. *International Journal for Numerical Methods in Engineering*, 72(12):1391–1433, 2007.

[13] C Linder and A Raina. A strong discontinuity approach on multiple levels to model solids at failure. *Computer Methods in Applied Mechanics and Engineering*, 253:558–583, 2013.